Comparison of ground-based GPS precipitable water vapour to independent observations and Numerical Weather Prediction model reanalyses over Africa.

O. Bock [1*], M.-N. Bouin [2], A. Walpersdorf [3], J.P. Lafore [4], S. Janicot [5], F. Guichard [4], A. Agusti-Panareda [6]

[1] *IPSL/SA, Université Paris VI, France*

[2] *LAREG, IGN, France*

[3] *LGIT, CNRS, France*

[4] *CNRM/GMME, Météo-France, France*

[5] *IPSL/LOCEAN, Université Paris VI, France*

[6] *ECMWF, Shinfield Park, Reading, England*

Submitted to:

Q. J. R. Meteorol. Soc.

Revised version from 12 October 2007

[*] Corresponding author: Institut Pierre Simon Laplace / Service d'Aéronomie, Université Paris VI, 4, place Jussieu, 75252 Paris cedex, France. E-mail: Olivier.Bock@aero.jussieu.fr

Summary

This study aims at assessing the consistency between different precipitable water vapour (PWV) datasets over Africa (between 10°S and 35°N). This region is characterized by large spatial and temporal variability of humidity but also by the scarcity of its operational observing network limiting our knowledge of the hydrological cycle. We inter-compare data from observing techniques such as ground-based Global Positioning System (GPS), radiosondes, AERONET sun photometers and SSM/I, as well as reanalyses from European Centre for Medium-Range Weather Forecasts (ERA40) and National Center for Environmental Prediction (NCEP2). The GPS data, especially, are a new source of PWV observation in this region. PWV estimates from nine ground-based GPS receivers of the international GPS network data are used as a reference dataset to which the others are compared. Good agreement is found between observational techniques, though dry biases of 12-14% are evidenced in radiosonde data at three sites. Reasonable agreement is found between the observational datasets and ERA40 (NCEP2) reanalyses with maximum bias ≤ 9% (14%) and standard deviation ≤ 17% (20%). Since GPS data were not assimilated in the ERA40 and NCEP2 reanalyses, they allow for a fully independent validation of the reanalyses. They highlight limitations in the reanalyses, especially at timescales from sub-daily to periods of a few days. This work also demonstrates the high potential of GPS PWV estimates over Africa for the analysis of the hydrological cycle, at timescales ranging between sub-diurnal to seasonal. Such observations can help studying atmospheric processes targeted by the African Monsoon Multidisciplinary Analysis (AMMA) project.

Keywords: GPS, precipitable water, Africa, Monsoon.

1. Introduction

Atmospheric water vapour is a key variable of the global climate system. It plays a crucial role in the radiative equilibrium, being the dominant greenhouse gas, and in climate change processes. Atmospheric water vapour is also an important component of the global hydrologic cycle. It shows significant variability, both in space and time over a large range of scales, resulting from the action of many atmospheric processes (transport, mixing, thermodynamics and microphysics) and interactions with the surface (evaporation of the oceans and evapotranspiration over land). Most meteorological processes (convection, cloud formation, precipitation) are influenced by local as well as large-scale variability in atmospheric water vapour.

In the present study, we will be interested in precipitable water vapour (PWV), which is the total atmospheric water vapour contained in a vertical column of unit area. This variable is strongly linked to the hydrological cycle and dynamical processes in the tropics where the overall PWV is high (Amenu and Kumar, 2005; Li and Chen, 2005). Since water vapour density is on the average quickly decreasing with altitude (with a scale height of ~2 km), PWV is closely related to lower tropospheric humidity. Most of the PWV variability is thus correlated with variability in the lower troposphere.

A number of observational techniques allow estimating the atmospheric PWV: either in-situ (e.g. radiosondes) or microwave and near-infrared or thermal infrared remote-sensing techniques (ground-based or spaceborne radiometers). Most of these techniques have limited retrieval capability (either only daytime operation or only over oceans), and thus their use for climate studies is limited or needs careful long-term data calibration (Amenu and Kumar, 2005). On the other hand, the combined use of these data has shown to improve Numerical Weather Prediction (NWP) model forecasts (Andersson et al., 2005).

Ground-based networks of Global Positioning System (GPS) form a new technique for the measurement of PWV observations. It relies on the observation of microwave signals transmitted from a constellation of high altitude (20,200 km) satellites. It is a differential technique and hence is much less subject to long-term calibration errors than other satellite remote sensing techniques. As the signals cross the atmosphere, they are delayed through refractive effects in the (dispersive) ionosphere and in the (neutral) troposphere. While the ionospheric delay is usually removed from the combination of dual frequency observations, the tropospheric delay needs to be estimated during GPS data processing (Bevis et al., 1992). The estimated tropospheric delay, referred to as zenith tropospheric delay (ZTD), is afterwards converted into PWV. Further details on the GPS retrieval technique will be given in section 2. To date, most studies using ground-based GPS PWV observations have been conducted at mid-latitudes where the accuracy of these observations was estimated to 1-2 kg m^{-2} (Rocken et al. 1995; Niell et al., 2001; Klein Baltink et al. 2002; Bock et al., 2005). A few experiments conducted in the tropics indicate slightly larger uncertainties (Takiguchi et al., 2000; Liou et al., 2001; Wu et al., 2003). In the tropics and especially over central and West Africa, there are at least two reasons why the accuracy of GPS PWV might be poorer: (i) the strong ionospheric activity around the magnetic equator and (ii) the scarcity of the permanent GPS network which leads to poorly determined GPS solutions (satellite orbits, stations coordinates and local reference frame). A careful analysis of the internal precision of GPS estimates (station coordinates and ZTD) over Africa is presented by Walpersdorf et al., 2007.

The motivation for the present work was to inter-compare and assess the accuracy of various PWV datasets in Africa for future water cycle studies in the framework of the African Monsoon Multidisciplinary Analysis (AMMA) project (http://www.amma-international.org/). The data from the sparse ground-based GPS network available over Africa in the period 1999-2005 are used here. Though many gaps are present in this dataset, it provides new and accurate observational data which are very useful for assessing more conventional datasets (radiosondes, sun photometers and SSM/I) and NWP model analyses. The African GPS network is intended to be enhanced within the AMMA project for period 2005-2007.

The organization of the paper is the following. Section 2 introduces the datasets and the methodology used for the inter-comparison. Section 3 presents the results from the observational techniques. Section 4 compares NWP model reanalyses to observations and provides some insight into the PWV variability as observed from GPS and NWP model reanalyses. Section 5 presents the conclusions and perspectives from the present work.

2. DATA AND ERROR SOURCES

(a) GPS data

For the present work we used data from nine ground-based GPS stations of the International GNSS Service (IGS) network (Beutler et al. 1999). The stations are located in the domain 25 °W – 45 °E by 10 °S – 35 °N (see Figure 1 and Table 1) and cover various climatic areas over Africa, from the Equator and the Tropics to the mid-latitudes. Most of them are located relatively close to the coast. The period of interest here is from January 1999 to July 2005. However, data are not available for all stations over the whole period since this network has been built up progressively. For example, only ASC1, MALI, and MAS1 have nearly continuous datasets since 1999 or before. Figure 2 shows the availability of GPS data and illustrates the various climatic features as seen from these PWV estimates. Though many gaps can be seen in these data series, these data are most welcome in that generally data-spare area, especially since they allow assessment of atmospheric water vapour, which is a crucial component of the tropical climate.

The ZTD dataset used in the present work is the final IGS product, which is a combination of ZTD estimates produced by up to 8 IGS analysis centres according to the procedure described by Gendt (2004). These data are available from ftp://garner.ucsd.edu/pub/troposphere/. The GPS ZTD estimates are produced with a 2 h time resolution, starting at 01 UT each day. Compared to a single processing, the combined product tends to be smoother (showing reduced temporal variability). It is also expected to have reduced bias, whereas a single processing can have biases up to ± 1 kg m^{-2} (Emardson et al. 1998; Niell et al., 2001; Klein Baltink et al. 2002; Bock et al., 2005; Walpersdorf et al., 2007).

The conversion of

GPS ZTD into PWV (hereafter, PWV^{GPS}) is performed in two steps (see, e.g., Bevis *et al.* 1994). Firstly, the contribution of dry air, referred to as zenith hydrostatic delay (ZHD) is evaluated at the location and time of the GPS observations and subtracted from ZTD. The calculation of ZHD is obtained from surface pressure, P^{surf}, at the height of the GPS receiver: ZHD = 2.279 [mm hPa^{-1}] $\times$ P^{surf} [hPa] / f(φ^{sta}, h^{sta}), where f(φ^{sta}, h^{sta}) is a correction of the mean gravity depending on the latitude, φ^{sta}, and altitude, h^{sta}, of the station (e.g. Klein Baltink et al. 2002; Hagemann et al., 2003). Secondly, the remainder is converted into PWV^{GPS} using a conversion factor $\kappa(T^m)$ as: $PWV^{GPS} = \kappa(T^m) \times (ZTD - ZHD)$. This factor depends on the water-vapour weighted mean temperature, T^m, in the column of atmosphere above the GPS antenna. It scales as ~ 155 kg m^{-3} under standard atmospheric conditions. Bevis *et al.* (1994), modelled $\kappa(T^m)$ as a linear function of surface temperature: $T^m = a \times T^{surf} + b$, with a = 0.72 and b = 70.2 K derived from a set of radiosonde data in the United States. Coefficients a and b are known to be season and latitude dependent (Ross and Rosenfeld, 1997). West Africa, and the tropics more generally, exhibit much smaller correlation between T^m and T^{surf}, and smaller seasonal cycle in a and b (Ross and Rosenfeld, 1997). We found values of a = 0.4 (0.5) and b = 174 (125) K from radiosonde data at Dakar (Libreville). Since only some of our GPS stations are collocated with radiosonde stations, we could not perform such a regression for all the GPS stations. We used thus the values derived by Bevis *et al.* (1994) at all stations. The root mean square (RMS) error associated with these values is estimated to ~4 K from radiosonde data at Dakar and Libreville. It might be responsible of errors up to 1.5% PWV, i.e. 0.5 – 1 kg m^{-2} with the present data. A more accurate station-dependent model for T_m should thus be used in future studies, such as fitted from NWP model analyses.

The surface pressure and air temperature required for the conversion of GPS ZTD estimates into PWV can be obtained either from an observing network (e.g. surface meteorological sensors) or a NWP model. Usually, these data need to be extrapolated or interpolated. The conversion has thus two additional error sources: (i) the extrapolation or interpolation method and (ii) the errors in the data (observations or model fields). According to the abovementioned relationship between *ZHD* and P_{surf}, an error of 1 hPa would produce an error of ~2.3 mm in ZHD (~ 0.35 kg m^{-2} in PWV). Hagemann *et al.* 2003, stressed that NWP surface pressure can deviate from surface observations by more than 3 hPa and thus recommended to use surface observational data instead of NWP model pressure fields. Bock et al., 2005, reported similar results and assessed additionally the uncertainty introduced by the vertical extrapolation of surface pressure and temperature when a simple thermodynamic formula is used (hydrostatic equilibrium and a constant temperature lapse rate of –6.5 K km^{-1}). This approach is shown to produce a RMS error less than 0.4 hPa in P_{surf} (~ 0.25 kg m^{-2} in PWV). Though these results suggest using surface observations instead of NWP model analyses, in the present work we use surface values from NCEP2 reanalysis (section 2.f). This choice was motivated by the fact that no surface observations were available nearby all GPS stations, and that ECMWF model reanalysis (ERA40) does not cover the whole period of interest. The operational analysis from ECMWF model has not been used because during the time period covered by the study, the configuration of the operational analyses changed, which could produce discontinuities in the surface fields. For the conversion, the nearest grid point from NCEP2 reanalysis is selected and pressure and temperature are extrapolated vertically to the altitude of the GPS stations (Bock et al., 2005). The 6-hourly NCEP2 data are interpolated to the time of the observations using a cubic-spline. The comparison of these data to radiosonde (4 sites) and surface observations (3 sites) show a mean (standard deviation) pressure error smaller than 1 hPa (1.5 hPa) and a temperature error smaller than 2 K (4 K).

Combining all the error sources mentioned in the preceding, the overall theoretical uncertainty associated with a single GPS PWV estimate is about ~ 1 – 2 kg m^{-2} RMS. This error estimate is consistent with previous studies comparing GPS PWV solutions with independent observing techniques such as radiosondes and microwave radiometers (Rocken et al. 1995; Emardson et al. 1998; Niell et al., 2001; Klein Baltink et al. 2002).

(b) Radiosonde data

Data from four radiosonde (RS) stations are used for a comparison with the GPS PWV over the period between January 1999 and July 2005. Their location and distance to the GPS stations is given in Table 1. They are identified through their World Meteorological Organization (WMO), five-digit codes. The time sampling of RS data was either once or twice a day, depending on the station: 61641 (00 and 12 UTC or 09 and 21 UTC), 60018 (00 and 12 UTC), 64500 (mainly 12 UTC, some at 09 UTC), and 60155 (00 UTC). The overlap with GPS dataset is the following: 05 Sept 2003 – 07 May 2005 for DAKA/61641, 01 November 2002 – 07 May 2005 for MAS1/60018, 08 June 2000 – 10 January 2004 for NKLG/64500, 02 March 2001 – 05 May 2005 for RABT/60155.

RS profiles containing pressure, temperature, and relative humidity were retrieved from the upper-air archive at the University of Wyoming (http://weather.uwyo.edu/upperair/sounding.html). They are composed of standard and significant levels. The RS PWV estimates, PWV^{RS}, have been recalculated from the profile data over the same depth of atmosphere as seen by the GPS receivers. Therefore, the integral of water vapour density was calculated between the altitude of a GPS station, $z^{\mathrm{surf,GPS}}$, and the highest altitude where humidity data are reported by the RS, $z^{\mathrm{top,RS}}$. In the case when $6 < z^{\mathrm{top,RS}} < 10$ km, a correction term (based on climatology) for the missing part above the profile has been added. This term was usually smaller than 1%. RS profiles where $z^{\mathrm{top,RS}} < 6$ km were discarded. When $z^{\mathrm{surf,GPS}}$ was below the altitude of the lowest data reported by the RS, $z^{\mathrm{surf,RS}}$, a correction term for the missing part of the bottom of the profile was also added (see Bock et al., 2005, for more details). Only RS profiles where $| z^{\mathrm{surf,RS}} - z^{\mathrm{surf,GPS}} | < 200$ m were retained. A number of additional quality-checks were also applied to every RS profile in order to detect outliers (which were evidenced from a careful inspection of this RS data set). A RS profile was retained only when: (i) upper and lower correction terms were smaller than 5 kg m^{-2}; (ii) $PWV^{\mathrm{RS}} < 70$ kg m^{-2}; (iii) $PWV^{\mathrm{RS}} < 1.5 \times PWV^{\mathrm{climat}}$, where PWV^{climat} is a PWV estimate from climatology (rescaled with the surface humidity from the RS profile).

However, despite these precautions, the accuracy of the RS dataset is difficult to assess. The four stations used in this study were equipped with Vaisala RS80 sensors over the period 1999-2005, except 60018 which was upgraded to Vaisala RS92 in 2005. The RS80 humidity sensor is known to have dry biases of up to 10% in specific humidity (Wang *et al.* 2002; Bock et al., 2005). However, in the total column humidity, dry biases are sometimes mitigated by wet biases due to contamination from rain and clouds. In order to eliminate cases where such a contamination is likely, RS PWV estimates have been filtered using the following procedure: (i) for each sounding, a saturation index is calculated as the integral of layers where relative humidity is above 95%; (ii) only profiles where this index is smaller than a prescribed threshold value are retained. This test has shown good performance with a threshold value set to 0.5 kg m^{-2} in Bock et al., 2005, and has been re-used here.

(c) Sun photometer data

Sun photometer (SPM) PWV products from the AErosol RObotic NETwork (AERONET, Holben et al., 1998) have been used for further intercomparison between with GPS and RS PWV data at two sites: Ascension Island (ASC1) and Dakar (DAKA). The AERONET SPMs observe solar radiation in various wavelengths in the visible and near infrared, including a water vapour line at 936 nm (Holben et al., 1998). They work during daytime only and data are screened for retaining mainly clear sky conditions. PWV is obtained using a differential absorption technique from the 936 nm line and nearby window wavelengths (see e.g., Halthore et al., 1997; Schmid et al., 2001). A comparison of SPM PWV to RS PWV showed an agreement of ± 10%, while the comparison of SPM PWV to microwave radiometer (MWR) PWV showed an agreement of ~5% (Halthore et al., 1997). An intercomparison between different SPMs has shown differences of ≤ 4.4% RMS, using standard procedures, while using the same radiative transfer model with all instruments, produce a spread of ≤ 8% RMS (Schmid et al., 2001). A further comparison with a MWR produced a similar difference of 8% RMS, or 2.2 kg m^{-2} in PWV (Schmid et al., 2001). The overall uncertainty in SPM PWV retrievals, such as produced from the AERONET network, is thus estimated to be smaller than ± 10% (Holben et al., 2001).

Level 1.5 (cloud-screened), version 2, AERONET PWV data have been retrieved from the NASA archive (http://aeronet.gsfc.nasa.gov/). The PWV data are reported every 15 minutes for elevation angles above 15°. Depending on the optical thickness of the atmosphere in the direction of the sun, the number of data points per day varied typically between zero (in case of obstruction of the sun by clouds or high aerosol load) and ~ 40 (in clear sky). In the region of interest, daytime observations run from 07 UTC to 19 UTC throughout the year. The GPS and AERONET dataset overlap is the following: 11 Jan 1999 – 17 Jun 2005 for ASC1 and 06 Sept 2003 – 31 July 2005 for DAKA. The AERONET PWV values have been corrected for the impact of difference in altitude with respect to the GPS receivers as described in sub-section 2.g. However, we observed small systematic differences when sun elevations were below 20-25°. We suspect these are due to variations in atmospheric transmittance at low elevations inducing biases in the AERONET PWV retrieval algorithm. These data were not excluded from the AERONET dataset.

(d) SSM/I data

The Special Sensor Microwave Imager (SSM/I) on board the Defense Meteorological Satellite Program (DMSP) satellites is a microwave radiometer operating in the 19, 22, 37 and 85-GHz frequency bands. Several DMSP satellites were orbiting during the period of interest, F13, F14, and F15 (the latter having been launched at the end of 1999). We used mainly data from the SSM/I onboard F13. This satellite crosses the Equator at 06:33 local solar time. It has a revisit period of 12-24 h (depending on the latitude considered), yielding thus one or two observations per day at the locations of the GPS stations. Higher diurnal sampling can be achieved from the combination of data from the other two satellites which are slightly delayed. The PWV product used here is that produced operationally by the NASA on a 0.25°-latitude by 0.25°-longitude grid, using the Wentz algorithm (Wentz, 1997). Presently, PWV is estimated accurately only over ocean regions in non-precipitating conditions. A comparison made with radiosonde observations from both small islands and ships has shown very good accuracy: -0.2 kg m^{-2} bias and 3.7 kg m^{-2} RMS difference (Deblonde and Wagneur, 1997).

For the intercomparison with GPS PWV data, only coastal and island stations were considered. The nearest pixel from SSM/I was selected, leading to median distances to GPS stations indicated in Table 1. The intercomparison periods are the following: 02 Jan 1999 – 25 Dec 2004 for ASC1, 05 Sept 2003 – 14 Jul 2004 for DAKA, 16 Aug 1999 – 30 Dec 2004 for MAS1, 21 Apr 2000 – 30 Dec 2004 for NKLG, and 15 Feb 2001 – 30 Dec 2004 for RABT. The SSM/I PWV data have been corrected for altitude difference with respect to the GPS receivers (see sub-section 2.g).

(e) ECMWF reanalysis

Global fields from the ERA40 reanalysis have been used for a systematic comparison at all GPS stations. The ERA40 archive is composed of 6-hourly global fields, with a horizontal resolution of 1.125° x 1.125° (Simmons and Gibson, 2000). The reanalysis covers the period from September 1957 to August 2002. There is thus only partial overlap with the GPS data available for Africa (e.g., no overlap with the Dakar GPS station which was installed in late 2002). PWV, temperature, T, and dew point temperature, Td, at 2 m have been extracted for each GPS station from the grid-point that minimized the difference in altitude within a horizontal distance of 100 km. The distance and difference in altitude for the selected grid points are reported in Table 1, where it is seen that the largest distance is 100 km and that the difference in height is smaller than 150 m for all stations. The extracted PWV data were further corrected for the difference in altitude (see sub-section 2.g). The GPS – ERA40 inter-comparison has been performed over the period 1999-2002.

For the period of interest here, the ERA40 analyses include, in addition to conventional data (e.g. radiosonde and surface SYNOP data), assimilation of satellite radiances from several instruments on the National Oceanic and Atmospheric Administration (NOAA) satellites as well as SSM/I PWV retrievals (Uppala et al., 2005). It has been shown that the global hydrological balance of the ERA40 analyses is not closed, especially since the assimilation of High Resolution Infrared Radiation Sounder (HIRS) and SSM/I satellite data (Andersson et al., 2005). The assimilation of these data led to a global increase in PWV (about 10%) and an increase in PWV increments (about 1% of total PWV added during each assimilation cycle). Most of the added moisture is afterwards rained out, leading thus to increased precipitation over the tropical oceans. This behaviour has been recognized as the major deficiency in the ERA40 system (Andersson et al., 2005). Among the possible reasons for this deficiency are: problems with the bias correction of satellite data, the vertical structure of humidity increments, and with the model's representation of tropical moist processes. Apart from model limitations, changes in the observing system also have been identified producing significant bias in climate variables. Bengtsson et al., 2004, showed that the decadal PWV trend was closer to observations when correcting ERA40 PWV for changes in the observing system. It is thus likely that the quality of PWV for the early periods is lower than that for later periods when satellite data were assimilated. Recent studies comparing ERA40 PWV to PWV observations yielded the following results: 2% (0.5 kg m^{-2}) dry bias compared to globally averaged ocean PWV from SSM/I (Andersson et al., 2005); general good agreement with slight dry biases compared to GPS PWV (Bengtsson et al., 2004; Hagemann et al., 2003); quite good reproduction of seasonal cycle but with a ~0 – 3 kg m^{-2} wet bias compared to merged MODIS and SSM/I PWV data (Li and Chen, 2005).

(f) NCEP-DOE reanalysis

The National Center for Environmental Prediction – Department of Energy (NCEP – DOE) reanalysis is an update to a former reanalysis of NCEP – National Center for Atmospheric Research (NCAR), with many problems corrected both in coding and data use (Kanamitsu et al., 2002). This reanalysis, referred to as NCEP2 in the following, used an improved forecast model and assimilation system, but humidity satellite data were not assimilated. The representation of upper-air humidity and PWV in NCEP2 is thus mainly constrained from radiosonde data. NCEP2 PWV data have been extensively compared to the NASA water VApor Project (NVAP) data at global scale by Amenu and Kumar (2005). These authors found that both datasets show qualitatively similar patterns in PWV, but that quantitatively there are considerable differences, both spatially and temporally. The discrepancies were mainly observed as a wetter atmosphere in NCEP2, on average, especially in winter months, with an overall smaller variability. A comparison of NCEP2 to ERA40 and merged MODIS/SSM/I observations over Australia and Asia also revealed some discrepancy in the seasonal cycle of PWV as represented in NCEP2 (Li and Chen, 2005).

NCEP2 fields are available on a 2.5° latitude x 2.5° longitude grid at 6-h temporal resolution. In the present work, NCEP2 PWV data from the nearest grid point to each GPS stations have been extracted. Due to the coarser resolution, the distance and difference in altitude with respect to the GPS stations is somewhat larger than with the ERA40 reanalysis (Table 1). The extracted PWV data were corrected for the difference in altitude (see below). The comparison has been performed over the period 1999-2005, which allowed inclusion of GPS station DAKA.

(g) Representativeness limitations and correction for difference in altitude

The inter-comparison of PWV estimates from different techniques is a good method for estimating the relative accuracy of the techniques. However, the results must be interpreted in the light of the representativeness of the various techniques. Generally speaking, large differences in representativeness can lead to serious limitation of the pertinence of any inter-comparison. The ground-based GPS technique provides PWV estimates representative of a horizontal scale of 20-50 km in the lower troposphere (assuming, e.g., observations down to 5° elevation angle and a water vapour scale height of 2-5 km). Compared to the in-situ observations taken by a radiosonde, the agreement can be as good as 1 kg m^{-2} when the RS balloon is launched nearby the GPS station (Bock et al., 2005). This good agreement is obtained because the two observations are spatially close in the lowest kilometres of the troposphere. A similar statement holds for the sun photometers since they sense a volume of atmosphere in a similar way as a GPS receiver (except they point only in the direction of the sun). The NWP model data, on the other hand, are representative of much larger spatial scales (~125 km for ERA40 and ~280 km for NCEP2). Hence, a perfect agreement between observations and NWP analyses is not to be expected.

Another source of uncertainty here is the impact of spatial displacement between sites and model grid-points. The correction of PWV estimates from the different datasets for horizontal and vertical displacement with respect to the GPS stations (taken here as a common reference dataset) requires the use of gridded data surrounding the various sites. This could be done using NWP model data. Because of the large difference in representativeness between the NWP models and observations, we limited the correction for the vertical displacement only; consistently with ECMWF's recommendation to the use the nearest model grid point (ideally extracted from the model's reduced Gaussian grid) for model validation against observations (Nurmi, 2003). For the correction of the vertical displacement, different methods have been tested. Following Bock et al., 2004, we first evaluated a scaling factor between PWV/PWV (the relative bias) and h the difference in altitude between the data points. A value close to – 40 % PWV per 1000 m is obtained during the wet seasons over Africa, consistent with the results of Bock et al., 2004, over Europe. However, due to the large seasonal cycle in PWV and marked variability during the dry season in the tropics (especially for Sahelian sites), a constant scaling factor was not adequate. Much better results were obtained when relating PWV to the humidity in the boundary layer rather than total PWV. For the present study, we use thus a simple model expressed as:

$$PWV = \quad {}_v h \cdot \left(1 - \frac{{}_v h}{2 \cdot PWV}\right),$$ where $_v$ is the water vapour density at the height of the reference (GPS) data point and h the difference in altitude between the data points. This model is derived analytically under the assumption of a linear decrease of water vapour

density in the troposphere. For the computation of $_{v}$ at the right altitude, T and Td at 2-m from NWP model analysis are extrapolated vertically assuming a constant lapse rate of -6.5 K km^{-1} and constant relative humidity. This kind of correction is very similar to that of Hagemann et al., 2003, but has the advantage of using only 2-m fields rather than model-level fields which require much larger disk space and computer time. For the correction of the ERA40 PWV estimates, we used T and Td fields from ERA40 analyses. For all other datasets, NCEP2 fields are used because their cover of the whole period of study. The magnitude of the correction is not shown here, but it can be inferred with a good accuracy from the – 40 % PWV per 1000 m rule of thumb. For tropical regions with an average PWV of 40 kg m^{-2} and a quite large difference in height of ± 200 m, the correction may reach ± 2.4 kg m^{-2}.

Note also that for all the inter-comparisons presented in sections 3 and 4, the data have been paired when they were closer than ± 1 hour on their original time grids (no PWV data are interpolated in time).

3. Intercomparison of PWV observations

(a) GPS compared to RS

In this section, GPS PWV is compared to PWV from RS data at four common sites. Table 2 shows the results of the comparison, in terms of bias (understood throughout this paper as the mean difference), standard deviation, correlation, and offset and slope parameters estimated from a linear least squares fit (PWV^{GPS} = slope $\times PWV^{RS}$ + offset) for either all data or 12-UTC data only. Figure 3 shows scatter diagrams which help interpreting slope and offset parameters reported in Table 2. The selected GPS and RS sites sample quite different climates. MAS1 (Mas Palomas Island) and RABT (Rabat, Morocco) are located near 30°N. The average PWV over the periods used in the comparison are 17.2 and 18.0 kg m^{-2}, at these stations respectively (Table 2). These are typical values for northern hemisphere extra-tropical stations. Figure 1 shows that the seasonal variability at both stations is quite large. DAKA (Dakar, Senegal) is located on the western coast of West Africa. The average PWV value is 24.9 kg m^{-2} (Table 2) and the seasonal variability is very large (see Figure 2). NKLG (N'Koltang – Libreville, Gabon) is an equatorial coastal station with a very high average PWV value of 45.6 kg m^{-2} (Table 2) and small seasonal variability (Figure 1a).

The mean difference and standard deviations at these four sites are quite different from one site to another (Table 2). Statistically significant large mean differences of more than 10%, are observed at DAKA, NKLG, and RABT. At MAS1 the mean difference is very small. At DAKA and RABT the mean difference is increasing when PWV is increasing. At NKLG, the mean difference is very large and nearly constant in range. Slope and offset parameters are not well constrained at this site because of the small excursion in PWV. The origin of these mean differences is further investigated below. It is shown that they are most likely due to dry biases in the RS humidity data.

Large standard deviations, of more than 10%, are observed at stations DAKA, MAS1, and RABT (Table 2). At DAKA, the offset parameter is close to zero while the slope parameter is significantly larger than one (its departure from one is much larger than for MAS1 and RABT). This indicates that there is an error source that is proportional to PWV. With the above-mentioned linear fit model, the standard deviation in $PWV^{GPS} - PWV^{RS}$ is reduced from 3.6 to 3.3 kg m^{-2} when the GPS data are corrected for the linear relation. When using the reverse linear model, PWV^{RS} = slope $\times PWV^{GPS}$ + offset, and fitting again slope and offset parameters, the standard deviation is even more reduced: from 3.6 to 2.8 kg m^{-2}. This indicates that there is an independent error source in RS PWV at Dakar. At MAS1 and RABT, neither such an effect nor gross outliers can be detected. It is possible that the comparison of PWV between GPS and RS at these stations is limited due to the horizontal distances (~ 100 km, see Table 1) separating the RS and GPS sites. This may especially limit the comparison at MAS1 (the GPS receiver is located on Mas Palomas Island, whereas the RS station is located on Tenerife island). Another possibility at that site may be the presence of a special error source in one of the data sets (for example multipath near the GPS antenna).

In addition to the overall statistics, we have investigated the inter-annual variations of yearly mean and standard deviations of GPS PWV – RS PWV. Figure 4a shows large variations in mean differences between years and sites. Some of this variability is due to different sampling of the different years (the time series are discontinuous) and different magnitudes of the seasonal cycles (Figure 2). In order to compensate for these artefacts, relative mean differences are also shown in Figure 4b, which yield higher coherence between years and sites. It highlights significant changes for some years. When discarding years with too few data (2000 for NKLG, 2001 for RABT, and 2002 for MAS1, using a threshold of 100 data pairs, see Figure 4d), we conclude on significant changes in mean difference at DAKA in 2003 (increased) and a continuous increase at RABT over 2002-2005. The particular results for DAKA in 2003 and large constant mean difference for NKLG are investigated below. The standard deviations are nearly constant and equal at all sites for all year (Figure 4c).

The impact on RS data of radiosonde time of launch has also been investigated. The lower part of Table 2 shows the GPS – RS differences when only 12 UTC data are used. The results are similar to the preceding at sites MAS1 and NKLG but not at DAKA. A closer inspection for additional time slots at this site revealed significant changes in the mean difference (offset parameter) depending on the time of day: +1.6 (-1.0) kg m^{-2} at 00 UTC, +4.5 (+0.2) kg m^{-2} at 09 UTC, +3.5 (-0.1) kg m^{-2} at 12 UTC, +2.6 (-1.5) kg m^{-2} at 21 UTC. There seems to be a significant increase of the mean difference during daytime at this site. This is consistent with the dry biases reported for this type of radiosonde humidity sensor (Vaisala RS80) in other regions by Wang et al., 2002.

(g) GPS and RS compared to AERONET sun photometers

In this section, GPS PWV estimates from stations ASC1 and DAKA are compared to PWV from collocated AERONET sun photometers. Table 3 shows the statistics of the comparison. A good agreement is found between GPS PWV and AERONET PWV at both stations, with an absolute value of the mean difference smaller than 2%, a standard deviation smaller than 12%, and a correlation larger than 0.96. The results do not change significantly when only data around 12 UTC are considered, hence giving confidence into the GPS PWV estimates throughout the diurnal cycle. The better agreement found for station ASC1 may be due to the smaller distance (3 km) between sites; at DAKA the distance is 63 km. It is likely that at coastal areas, such a large distances can lead to significantly different observations of PWV from both sites. The agreement between PWV estimates from GPS and AERONET is consistent with previously published results using AERONET data (see section 2c).

Table 3 shows that the agreement between GPS and AERONET observations is much higher than that obtained between RS and GPS. Inspection of the PWV data from all three datasets at Dakar, Figure 5, reveals a large discrepancy in RS PWV compared to both GPS and AERONET PWV. In September and October 2003, the mean difference between GPS PWV and RS PWV is 9.0 and 7.0 kg m^{-2}, respectively, while it is only –0.05 and –0.63 kg m^{-2} for GPS PWV compared to AERONET PWV. From November 2003 on, all three datasets agree well. We noticed that on early September 2003, the sounding hours at Dakar were switched from 00 and 12 UTC to 09 and 21 UTC. The sounding times were then switched again to 00 and 12 UTC in April 2004. The large mean difference observed during September and October 2003, combined with the change of launch time, let us assume that a change in sounding procedure is probably at the origin of the large dry bias seen in the RS data. A secondary effect might be the different sampling times of the diurnal cycle (a combined effect of a change in RS dry bias, such as due to sensor arm heating, and a change in the properties of the atmosphere itself, such as more water vapour, presence of clouds…).

(h) GPS and RS compared to SSM/I

In this section, GPS PWV estimates from five coastal sites are compared to PWV estimates from SSM/I. Table 4 shows the statistics of the comparison. Overall there is a good agreement, with mean differences below 8% and correlations above 0.87. This demonstrates that the PWV fluctuations at timescales larger than 12 to 24 h (which is the sampling time of SSM/I at a fixed location) are properly measured by both techniques. The high correlation is mainly due to the large spatial scale of the strongest PWV fluctuations (already observed at mid-latitudes by Bock et al., 2005). These results are consistent with previously published comparisons between SSM/I and other techniques (see section 2d). The largest mean differences are observed at DAKA and MAS1, indicating wet biases in SSM/I data. The largest standard deviations ($\geq$2.2 kg m^{-2}) are observed at MAS1 at highest altitude above mean sea level and the sites located at 100 km or more from the coast (NKLG and RABT). These may be limited by representativeness differences in both datasets. The very small mean differences observed at sites NKLG and RABT further sustain the hypothesis for dry biases in the RS data from the corresponding sites. Figure 6 illustrates the PWV series observed with GPS, RS and SSM/I at site NKLG for a full seasonal cycle. The rather good agreement between GPS and SSM/I is contrasting with the large mean difference and scatter in the RS data.

In this section we showed that all four datasets are capable of providing an accurate description of PWV variability, though some dry and wet biases are found in some datasets (RS and SSM/I, especially). The various results between techniques are illustrated in Figure 7. All the RS data used in this study showed dry biases. The AERONET sun photometer (SSM/I) data show very good agreement with GPS at the two (five) sites used here and provide accurate PWV estimates during daytime (over ocean). The main advantage of the ground-based GPS technique are that it covers a broad range of timescales, from sub-diurnal to multi-annual, and that data are available in all weather conditions. Its main limitation is the poor spatial coverage.

4. NWP MODEL RE-ANALYSES COMPARED TO OBSERVATIONS

(a) ERA40

Table 5 shows the statistics of the comparison between ERA40 PWV and GPS PWV estimates for all sites except DAKA for which there was no overlap with the ERA40 dataset. Good agreement is found at all stations. The absolute mean difference is smaller than 9% and the standard deviation is better than 17%. The smallest correlations are observed at equatorial sites, especially MBAR and MSKU. The equatorial sites have also the largest offsets and their slopes are differing significantly from one. This is partly due to the small excursion in PWV which weakly constrained linear fit parameters (Figure 3).

Based on mean difference and standard deviation criteria, the overall agreement between the ERA40 analysis and GPS observations is nearly similar to that between GPS and RS or SSM/I. This is not surprising knowing that RS and SSM/I data are assimilated into the ERA40 analysis. A detailed inspection, for a subset of sites, shows however some interesting differences. The GPS – RS comparison (Table 2) pointed out large dry biases in the RS data from Libreville (NKLG), Dakar (DAKA), and Rabat (RABT). The GPS – SSM/I comparison (Table 4), showed quite good agreement between both datasets, with slight wet biases in SSM/I data at sites DAKA and MAS1. One interesting question is: how well does the assimilation system manage these two datasets with contrasting biases? A careful inspection of statistics from the ERA40 assimilation reports, the “feedback files”, for the period 1999-2002 has revealed much interesting information, see Table 6. Overall, the mean observation minus background (background departure) at all four radiosonde sites shows a large dry bias, in the range -1.5 to -2.4 g kg^{-1}, at the lowest level (1000 hPa). Libreville, Dakar and Rabat show a maximum bias at 925 hPa and, in addition, a large dry bias at upper levels (300 hPa). All stations show large humidity data rejection at the 1000 hPa level (only 26% used for Libreville), which is mainly due to blacklisting (the condition for blacklisting is that the pressure level of the observed humidity is smaller than the model surface pressure minus 4 hPa). Background departures are often taken as an estimate of observing system errors. If we use the o-b humidity bias integrated over the 1000-850 hPa as an estimate of the RS PWV bias, we see that we obtain consistent results with Table 2 (though this reduced vertical range may not account exactly for the total column PWV bias). If we compare now the o-b and o-a bias, we see that the assimilation system gives a significant weight to the RS data (the o-a bias is reduced). The analysis increment (a-b difference) indicates that the analysis is drier than the background by 0.7 to 1.4 kg m^{-2}, most likely as a result of the assimilation of the too dry RS data. However, the mean difference between RS data and analysis (o-a bias) is still -0.8 to -1.4 kg m^{-2}. This difference suggests that other assimilated data with significant weight counterbalance the too dry RS data. Andersson et al., 2006, showed that surface data (SYNOP) and SSM/I data have significant impact on the analysed humidity fields over land and ocean, respectively. Similarly, the slight wet bias in SSM/I PWV data may explain the o-a PWV bias. Overall, the combined use of SYNOP, RS and SSM/I data (among others) leads to quite small biases in the ERA40 analysis as compared to the GPS PWV estimates. The 1.1 and 1.5 kg m^{-2} biases observed at NKLG and MSKU, respectively, compared to GPS PWV (Table 5) are fairly consistent with the analysis increment at Libreville (Table 6). The -1.4 kg m^{-2} wet bias observed at ASC1 is also consistent with the SSM/I wet bias (Table 4), but the large dry bias at MALI is not explained.

Tables 2, 4 and 5 show also that, at the common sites, GPS – ERA40 differences show similar or higher standard deviation and smaller correlation than the differences between GPS and the other two observational techniques. This poorer agreement suggests that ERA40 reanalysis contains some additional noise or independent fluctuations. These spurious fluctuations may be due either to the difference in representativeness between this dataset and the GPS dataset, to time varying errors in the data assimilated (e.g. RS daytime dry bias), and/or to difficulties for the model to represent properly the processes involved in the shorter time-scale fluctuations (e.g. complex surface-atmosphere interactions that are not modelled in ERA40). Figure 8 shows daily mean data at six sites over a complete seasonal cycle. It is seen that large discrepancies (up to 10 kg m^{-2} between GPS and ERA40) occur at time scales of 1-10 days, especially at equatorial sites (MALI, MBAR, and NKLG). The reanalysis seems to have a tendency to exaggerate the magnitude of rapid PWV variations. At the other sites, this effect is less marked (see e.g. comparison with SSM/I in Figure 6). On the other hand, it is seen, at the sites where GPS data are available, that the seasonal evolution of ERA40 PWV is close to that of the GPS PWV.

(i) NCEP2

In this section, GPS PWV is compared to PWV from NCEP2 at all GPS stations for the period 1999-2005. Table 7 shows the statistics of the comparison on the basis of 6-hourly data. The overall dry bias in NCEP2 PWV is consistent with the findings of Amenu and Kumar, 2005, for equatorial and northern tropical regions. Compared to the ERA40 results (Table 5), the agreement between NCEP2 PWV and GPS PWV is significantly lower. Overall, the standard deviations are in the range 11 – 20% (with an average of 16% compared to 11% for ERA40), mean differences in the range -8 to +14% (with an average of +4% compared to +1% for ERA40), and correlations in the range 0.50 – 0.93 (with an average of 0.67 compared to 0.81 for ERA40). The smaller correlation found at equatorial sites is again a result of the smaller seasonal cycle at these sites. However, on a site by site basis, these results are highly consistent with those obtained with ERA40: mean differences and standard deviations are observed at the same sites, though being magnified in NCEP2. Similarly to ERA40, the seasonal cycle is overall quite well reproduced in NCEP2, though its amplitude is slightly too small (consistently with Amenu and Kumar, 2005, and Li and Chen, 2005). Similarly also, large discrepancies (up to 20 kg m^{-2}) are seen at timescales of 1-10 days in NCEP2 compared to GPS or ERA40 PWV.

There are several reasons that may explain the large differences observed between NCEP2 and the other datasets. An obvious one is the looser horizontal grid resolution, increasing representativeness differences, especially at coastal sites. A subtler one may come from data assimilated in the NCEP2 reanalyses. The NCEP2 reanalysis uses very limited satellite data, and especially not the SSM/I data (Kanamitsu et al., 2002). The humidity fields in the NCEP2 reanalysis are thus strongly dependent on RS data and model physics where no upper air humidity data are available. An example of dry bias transferred from RS data to the reanalysis is seen at Libreville/NKLG in Figure 6 and 8. There is a strong correlation between the NCEP2 time series and the RS time series at that site and the dry bias in NCEP2 is fairly consistent with the RS dry bias discussed above. A similar example can be found at Dakar during September-October 2003 when the RS data showed a large dry bias (section 3). Another probable reason for the difference may come from limitations in model parameterizations in the data sparse region considered here. Similar impact of RS biases and limitations in model physics in the NCEP2 reanalysis have been reported by Sudradjat et al., 2005.

(j) Discussion on PWV variability in reanalyses

In the previous sub-sections, differences in PWV from the two reanalyses and observations have been evaluated at the full time resolution of the reanalyses, i.e. 6-hourly. It has been noticed from Figure 8 that most of the discrepancy between the datasets is due to spurious fluctuations at timescales of 1-10 days or less. The diurnal cycle, also, is expected to contribute to a non negligible part of the observed standard deviation, as it is generally recognized that NWP models have difficulty in representing it in the tropics (Yang and Slingo, 2001). In order to evaluate more precisely the contribution of different timescales to the observed differences, which may be related to distinct atmospheric processes, we averaged the data on daily and weekly periods. Table 8 shows the mean results (averaged over all sites) for both reanalyses. It is seen that the standard deviation decreases and the correlation increases as the averaging period increases. For ERA40, 20% of the standard deviation is due to sub-diurnal fluctuations and nearly 50% to timescales smaller than 7 days. For NCEP2, these fractions are smaller (10% and 36%, respectively), indicating that the latter reanalysis has also difficulty in representing synoptic and larger-scale variability (i.e. at timescales larger than 7 days). The reduction in standard deviation is observed at all sites in both reanalysis, but is especially marked at equatorial sites.

The GPS data, through their high temporal resolution, offer a unique possibility to investigate the diurnal cycle in PWV and evaluate the reanalyses at this timescale. The inspection of GPS PWV data revealed actually marked diurnal cycles at most sites, consistently with Wu et al., 2003. Some of them showed a strong 24-h periodicity, while others had also a strong semi-diurnal component. Strong 24-h periodicity was found at continental sites (MBAR, MSKU and YKRO). The semi-diurnal oscillation was more often observed at equatorial sites during the wet seasons (NKLG, MSKU, MALI). Other sites like DAKA, RABT and ASC1 did not exhibit marked diurnal oscillations. At Dakar, especially, large PWV modulations were observed at longer timescales throughout the year (see Figure 5 and 8) with little phasing with the diurnal cycle. The large fluctuations with periodicities in the 3-9 day range may be linked with African Easterly Waves during the wet season (Diedhiou et al., 1999), while the longer ones, in the range 10-40 days, may be linked with the Madden-Julian intra-seasonal oscillation (Matthews, 2004; Mounier and Janicot, 2004). More investigation is needed to establish the impact of these synoptic to global scale disturbances on PWV and humidity fluxes over West Africa.

5. Conclusion and perspectives

This study aimed at comparing various datasets of PWV available over Africa, in view of their use for water cycle studies in the framework of the AMMA project. The quantitative inter-comparison has been performed with respect to ground-based GPS PWV data from nine IGS stations. Therefore, the other datasets have been corrected for the vertical displacement with respect to the GPS stations. In a first part, ground-based GPS PWV data have been compared to PWV estimates from other observational techniques: RS (at 4 sites), AERONET sun photometers (at 2 sites), and SSM/I (at 5 coastal sites). A good agreement was found (mean difference ≤ 2%, standard deviation ≤ 12%) between GPS and AERONET sun photometers; as well as between GPS and SSM/I (mean difference ≤ 8%, standard deviation ≤ 15%). These results are consistent with those of Takiguchi et al., 2000, and Liou et al., 2001, using GPS data in tropical regions. On the other hand, significant dry biases were found (12-14%) in RS data from Libreville, Dakar and Rabat, consistently with Wang et al., 2002, over the tropical oceans. Table 9 gives a summary of results (averaged over all the sites). Overall, RS data show a dry bias of 3.2 kg m^{-2} (and standard deviation of 3.0 kg m^{-2}) compared to GPS. The SSM/I data show a wet bias of -0.6 kg m^{-2} (and standard deviation of 2.1 kg m^{-2}) compared to GPS.

In a second part, PWV data from ERA40 and NCEP2 reanalyses have been compared to the observational data. However, only the GPS data are fully independent since radiosonde data are assimilated in both reanalyses and SSM/I data are assimilated in ERA40 only. Overall, both reanalyses have been shown to reproduce well the seasonal cycle in PWV. Using full-resolution data (6-hourly), ERA40 is shown to agree quite well with GPS data (mean difference ≤ 9%, standard deviation ≤ 17%), while NCEP2 showed lower performance (mean difference ≤ 14%, standard deviation ≤ 20%). The biases observed in both reanalyses have been shown to be partly related to dry biases detected in the RS data (in accordance with Sudradjat et al., 2005) and partly to wet biases in the SSM/I data (for ERA40). Table 9 gives the mean and standard deviation of the difference between observations and reanalyses limited to the period of ERA40 (section 2.e) for both reanalyses. The mean difference between the reanalyses indicates NCEP2 is drier by 1.5 kg m^{-2} than ERA40. Both reanalyses are too dry compared to GPS and too wet compared to RS (due to RS dry bias). The agreement with SSM/I is quite good, but the sign of the mean difference depends on the reanalysis. For ERA40 it has also be shown that the model background departure (RS observation minus background used in the assimilation system) was consistent with GPS departure (RS minus GPS) and may thus be used for the detection of RS biases.

While most previous studies intercompared ERA40 and NCEP2 PWV fields or compared them to observations on a monthly average basis, we have here investigated shorter timescales (from 6-hourly to a few days). In the period range from one day to ten days or more, ERA40 performs better than NCEP2, especially at coastal sites. This might be due to the positive impact of assimilation of satellite data over the oceans in ERA40 (in accordance with Andersson et al, 2006). Nevertheless, we noticed that both models have a tendency to exaggerate PWV fluctuations at synoptic timescales.

These results point thus to limitations in the reanalyses for studying the water cycle in the tropics (in accordance with Sudradjat et al., 2005, and Li and Chen, 2005). The limitations seem to be more severe for NCEP2 than for ERA40. These results confirm also the high potential of GPS data for estimating PWV at a broad range of timescales over Africa. A more in-depth analysis of the seasonal cycle, inter-annual and intra-seasonal variability, as well as diurnal cycle in GPS PWV data is presently under investigation.

A major perspective of this work is the development and use of a GPS network over West Africa in the framework of the AMMA project (http://amma-international.org/). This network will cover the region in between 9.5°N and 16.5°N around the Greenwich Meridian. These GPS data will allow monitoring the seasonal cycle in PWV, and investigate the processes linked to the onset and retreat of the monsoon, as well as its intra-seasonal variability (dry/wet monsoon surges). It will also enable to analyze the diurnal cycle which is known to be strongly connected with the meridional vegetation gradient and low level monsoon flux (Mohr, 2004; Parker et al., 2005). The new GPS data will also enable to further evaluate and improve the water cycle in NWP models over the Sahel.

ACKNOWLEDGEMENTS

The authors acknowledge the insightful comments and suggestions from two anonymous reviewers that helped improving the analysis and presentation of these results. The authors would like to acknowledge the efforts of the people participating in the establishment and maintenance of the observational networks used in the present study: the international GPS network, the RS stations (mainly run by national meteorological offices and Agence pour la Sécurité de la Navigation Aérienne, ASECNA), the AERONET network (especially the principal investigators of Ascension Island and Dakar sites, Brent Holben and Didier Tanré, respectively). The authors acknowledge also the people involved in the data processing and management of databases: IGS analyses centres for GPS data, Institut Pierre Simon Laplace for archiving ERA40 reanalyses and SSM/I data, and NOAA for the NCEP2 database. The authors thank G. Gendt, GFZ, for information provided on the IGS ZTD product, L. Isaksen, D. Dee, S. Uppala, and E. Andersson, ECMWF, for their software and advice on producing ERA-40 statistics, and J. Tarniewicz, NOVELTIS and IPSL, for preparing the SSM/I data. The authors would like to specially thank J.L. Redelsperger, CNRS/CNRM, for strong support for the development of the GPS component in AMMA. Based on French initiative, AMMA was built by an international scientific group and is currently funded by a large number of agencies, especially from France, UK, US and Africa. It has been the beneficiary of a major financial contribution from the European Community's Sixth Framework Research Programme. Detailed information on scientific coordination and funding is available on the AMMA International website http://www.amma-international.org.

References

Amenu G, Kumar P. 2005. NVAP and Reanalysis-2 global precipitable water products. Intercomparison and variability studies. *Bull. Am. Meteorol. Soc.* **86**: 245–256.

Andersson E, et al. 2005. Assimilation and Modeling of the Atmospheric Hydrological Cycle in the ECMWF forecasting system. *Bull. Am. Meteorol. Soc.* **86**: 387–402.

Andersson E, Holm E, Bauer P, Beljaars A, Kelly GA, McNally AP, Simmons AJ, Thepaut JN, Tompkins AM. 2007. Analysis and forecast impact of the main humidity observing systems. *Q. J. R.. Meteorol. Soc.*. **133:** 1473—1485. DOI: 10.1002/qj.112

Bengtsson L, Hagemann S, Hodges KI. 2004. Can climate trends be calculated from reanalysis data? *J. Geophys. Res.* **109**. DOI: 2004JD004536.

Beutler G, Rothacher M, Schaer S, Springer TA, Kouba J, Neilan RE. 1999. The International GPS Service (IGS): An Interdisciplinary Service in Support of Earth Sciences. *Adv. Space Res.* **23**: 631–635.

Bevis M, Businger S, Herring TA, Rocken C, Anthes RA, Ware RH. 1992. GPS Meteorology: Remote Sensing of the Atmospheric Water Vapour Using the Global Positioning System. *J. Geophys. Res.* **97**: 15787–15801.

Bevis M, Businger S, Chiswell S, Herring TA, Anthes RA, Rocken C, Ware RH. 1994. GPS Meteorology: Mapping zenith wet delay onto precipitable water. *J. Appl. Meteorol.* **33**: 379–386.

Bock O, Flamant C, Richard E, Keil C, Bouin MN. 2004. Validation of precipitable water from ECMWF model with GPS data during the MAP SOP. 11th conference on mountain meteorology, 21–25 June 2004, Bartlett, NH.

Bock O, Keil C, Richard E, Flamant C, Bouin MN. 2005. Validation of precipitable water from ECMWF model analyses with GPS and radiosonde data during the MAP SOP, *Q. J. R.. Meteorol. Soc.* **131**: 3013–3036.

Deblonde G, Wagneur N. 1997. Evaluation of global numerical weather prediction analyzes and forecasts using DMSP special sensor microwave imager retrievals. 1. Satellite retrieval algorithm intercomparison study. *J. Geophys. Res.* **102**: 1833-1850.

Diedhiou A, Janicot S, Viltard A, de Felice P, Laurent H. 1999. Easterly wave regimes and associated convection over West Africa and tropical Atlantic: results from the NCEP/NCAR and ECMWF reanalyses. *Climate Dyn.* **15:** 795-822.

Gendt G. 2004. Report of the tropospheric working group for 2002. IGS 2001-2002 Technical Report, Jet Propulsion Laboratory, Pasadena, Publ. 04-017, Sept 2004, p.209-212, available from http://igscb.jpl.nasa.gov/igscb/resource/pubs/0102TR/2001-2002_tech_report.pdf.

Hagemann S, Bengtsson L, Gendt G. 2003. On the determination of atmospheric water vapour from GPS measurements . *J. Geophys. Res.* **108 (D21)**: 4678.

Halthore RN, Eck TF, Holben BN, Markham BL. 1997. Sun photometric measurements of atmospheric water vapour column abundance in the 940-nm band. *J. Geophys. Res.* **102(D4)**: 4343-4352.

Holben, BN, Eck TF, Slutsker I, Tanre D, Buis JP, Setzer A, Vermote E, Reagan JA, Kaufman YJ, Nakajima T, Lavenu F, Jankowiak I, Smirnov A. 1998: AERONET: A federated instrumented network and data archive for aerosol characterization. *Remote Sens. Environ.,* **66:** 1–16.

Holben, BN, Tanre D, Smirnov A, Eck TF, Slutsker I, Abuhassan N, Newcomb WW, Schafer J, Chatenet B, Lavenu F, Kaufman YJ, Vande Castle J, Setzer A, Markham B, Clark D, Frouin R, Halthore R, Karnieli A, O'Neill NT, Pietras C, Pinker RT, Voss K, Zibordi G. 2001. An emerging ground-based aerosol climatology: Aerosol Optical Depth from AERONET. *J. Geophys. Res*. **106**: 12 067-12 097.

Kanamitsu M, Ebisuzaki W, Woollen J, Yang SK, Hnilo JJ, Fiorino M, Potter GL. 2002. NCEP – DOE AMIP-II Reanalysis (R-2). *Bull. Am. Meteorol. Soc.* **83**: 1631-1643.

Klein Baltink H, van der Marel H, van der Hoeven AGA. 2002. Integrated atmospheric water vapour estimates from a regional GPS network. *J. Geophys. Res.* **107(D3)**. DOI: 10.1029/2000JD000094.

Li H, Chen B. 2005. The evolution of precipitable water associated with the Asian and Australian monsoons as revealed from MODIS/SSM/I, ECMWF and NCEP reanalysis data sets. *Geophys. Res. Lett.* **32**. DOI:10.1029/2005GL022570.

Liou YA, Teng YT, Van Hove T, Liljegren JC. 2001. Comparison of Precipitable Water Observations in the Near Tropics by GPS, Microwave Radiometer, and Radiosondes. *J. Appl. Meteorol.* **40:** 5-15.

Matthews A. 2004. Intraseasonal Variability over Tropical Africa during Northern Summer. *J. Climate*. **17:** 2428-2440.

Mohr K. 2004. Interannual, Monthly, and Regional Variability in the Wet Season Diurnal Cycle of Precipitation in Sub-Saharan Africa. *J. Climate*. **17:** 2441-2453.

Mounier F, Janicot S. 2004. Evidence of two independent modes of convection at intraseasonal timescale in the West African summer monsoon. *Geophys. Res. Lett.* **31**. DOI:10.1029/2004GL020665.

Niell AE, Coster AJ, Solheim FS, Mendes VB, Toor PC, Langley RB, Upham CA. 2001. Comparison of Measurements of Atmospheric Wet Delay by Radiosonde, Water Vapour Radiometer, GPS, and VLBI. *J. Atmos. Oceanic Technol*. **18**: 830–850.

Nurmi P. Recommendations on the verification of local weather forecasts, ECMWF Technical Memo. 430, 19 pp., December 2003 (available from http://www.ecmwf.int/publications/library/ecpublications/_pdf/tm/401-500/tm430.pdf).

Parker DJ, Burton RR, Diongue-Niang A, Ellis RJ, Felton M, Taylor CM, Thorncroft CD, Bessemoulin P, Tompkins AM. 2005. The diurnal cycle of the West African monsoon circulation. *Q. J. R.. Meteorol. Soc..*. **131:** 2839-2860.

Rocken C, VanHove T, Johnson J, Solheim F, Ware RH, Bevis M, Chiswell SR, Businger S. 1995. GPS/STORM-GPS sensing of atmospheric water vapour for meteorology. *J. Atmos. Oceanic Technol*. **12**: 468-478.

Ross RJ, Rosenfeld S. 1997. Estimating mean weithed temperature of the atmosphere for Global Positioning System applications. *J. Geophys. Res*. **102(D18)**: 21719 – 21730.

Schmid B, Michalsky JJ, Slater DW, Barnard JC, Halthore RN, Liljegren JC, Holben HB, Eck TF, Livingston JM, Russell PB, Ingold T, Slutsker I. 2001. Comparison of columnar water vapour measurements during the fall 1997 ARM Intensive Observation Period: solar transmittance methods. *Appl. Opt.* **40:** 1886–1896.

Simmons AJ, Gibson JK. 2000. The ERA40 project plan, ERA40 Proj. Rep. Ser. 1, 62 pp., Eur. Cent. for Medium-Range Weather Forecasts, Reading, U. K.

Sudradjat A, Ferraro RR, Fiorino M. 2005. A Comparison of Total Precipitable Water between Reanalyses and NVAP. *J. Climate*. **18:** 1790–1807.

Takiguchi H, Kato T, Kobayashi H, Nakaegawa T. 2000. GPS observations in Thailand for hydrological applications. *Earth, Planets and Space*. **52**: 913-919.

Uppala SM and 45 co-authors. 2005. The ERA-40 Reanalysis. *Q. J. R.. Meteorol. Soc.*, **131**,

Walpersdorf A, Bouin MN, Bock O, Doerflinger E. 2007. Assessment of GPS data for meteorological applications over Africa: Study of error sources and analysis of positioning accuracy. *J. Atmos. Solar Terrestrial Phys.* **69:** 1312–1330.

Wang J, Cole HL, Carlson DJ, Miller ER, Beierle K, Paukkunen A, Laine TK. 2002. Corrections of humidity measurement errors from the Vaisala RS80 radiosonde - Application to TOGA_COARE data. *J. Atmos. Oceanic Technol.* **19:** 981-1002.

Wentz F. 1997. A well calibrated ocean algorithm for Specila Sensor Microwave/Imager. *J. Geophys. Res.* **102(C4)**: 8703-8718.

Wu PM, Hamada JI, Mori S, Tauhid YI, Yamanaka MD, Kimura F. 2003. Diurnal variation of precipitable water over a mountainous area of Sumatra Island. *J. Appl. Meteorol*. **42**: 1107– 1115.

Yang GY, Slingo J. 2001. The diurnal cycle in the tropics. *Mon. Weather Rev.* **129:** 784-801.

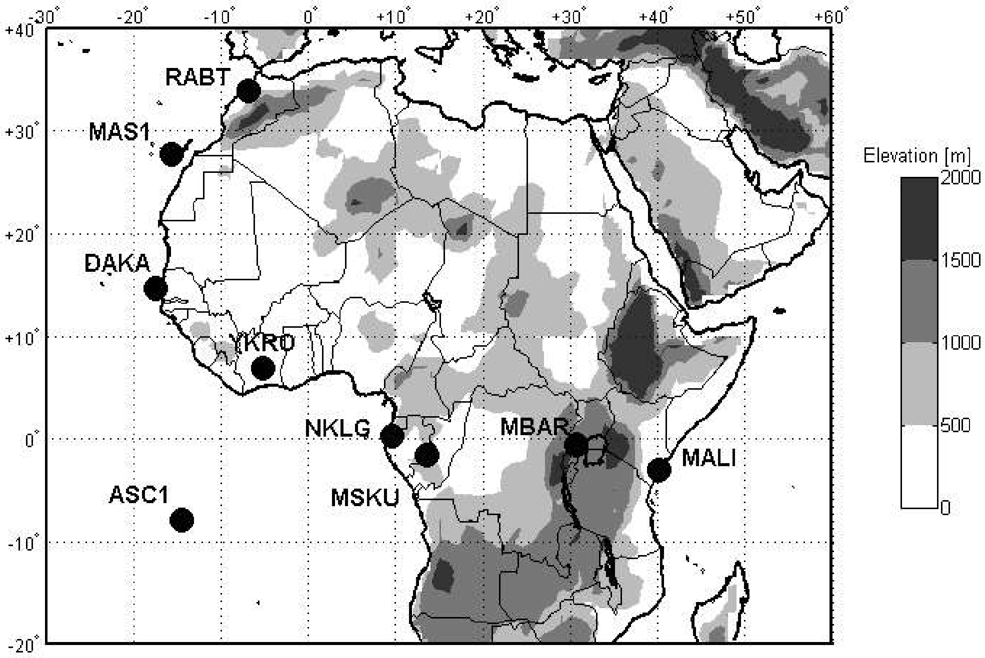

Fig. 1: Map of the domain of study with GPS stations indicated as black circles with four-letter names (9 stations). Gray shading represents surface elevation with the scale indicated on the right.

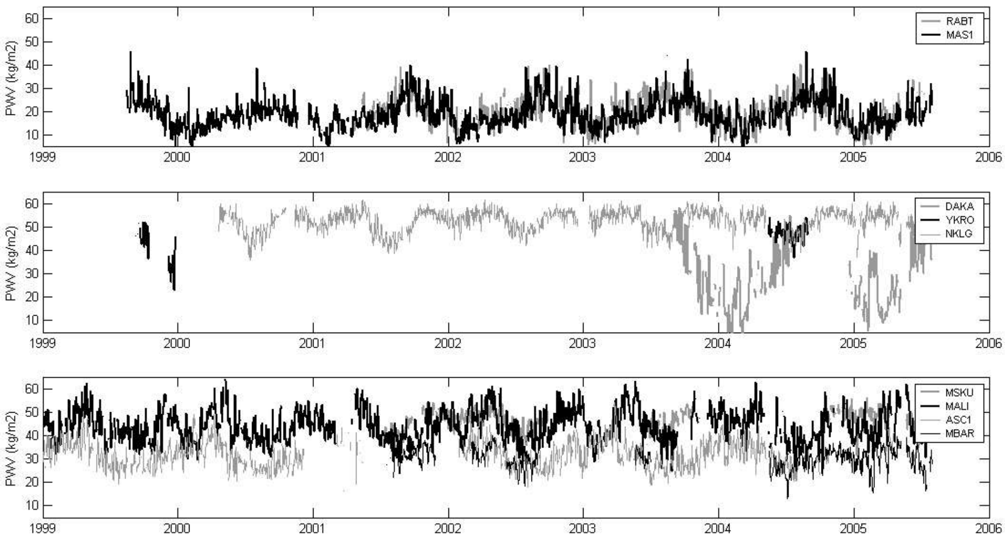

Fig. 2: Time series of PWV estimates from ground-based GPS receivers: (upper plot) northern extra-tropical stations (RABT and MAS1); (middle plot) West Africa stations (DAKA, YKRO, NKLG); (lower plot) equatorial stations (MSKU, MBAR, MALI) and southern hemisphere tropical station (ASC1).

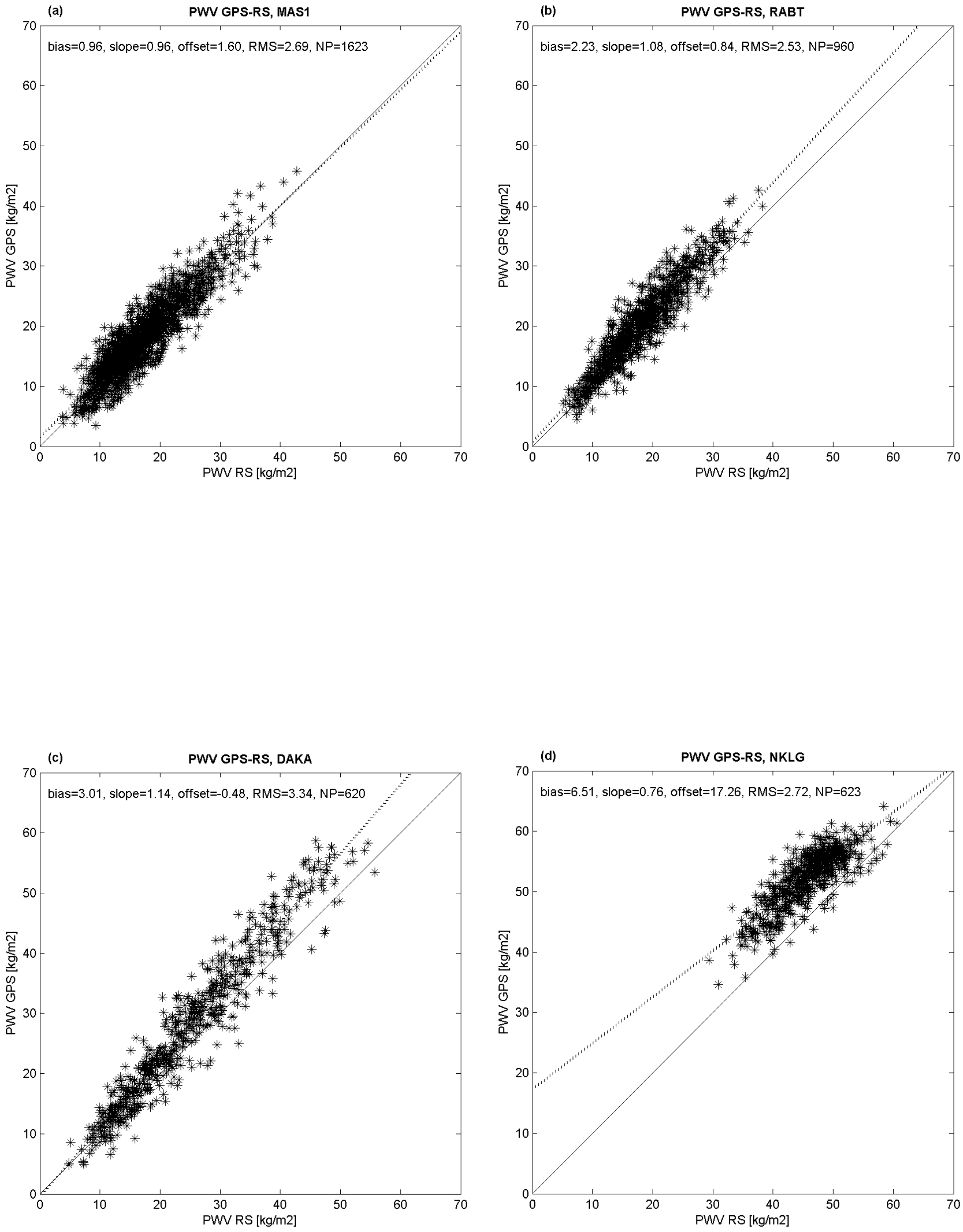

Fig. 3. Scatter diagrams of PWV from GPS compared to radiosonde stations (RS) at four stations: (a) RABT, (b) MAS1, (c) DAKA, (d) NKLG. Best fit lines are indicated as dotted lines. See Table 2, for the corresponding fit parameters.

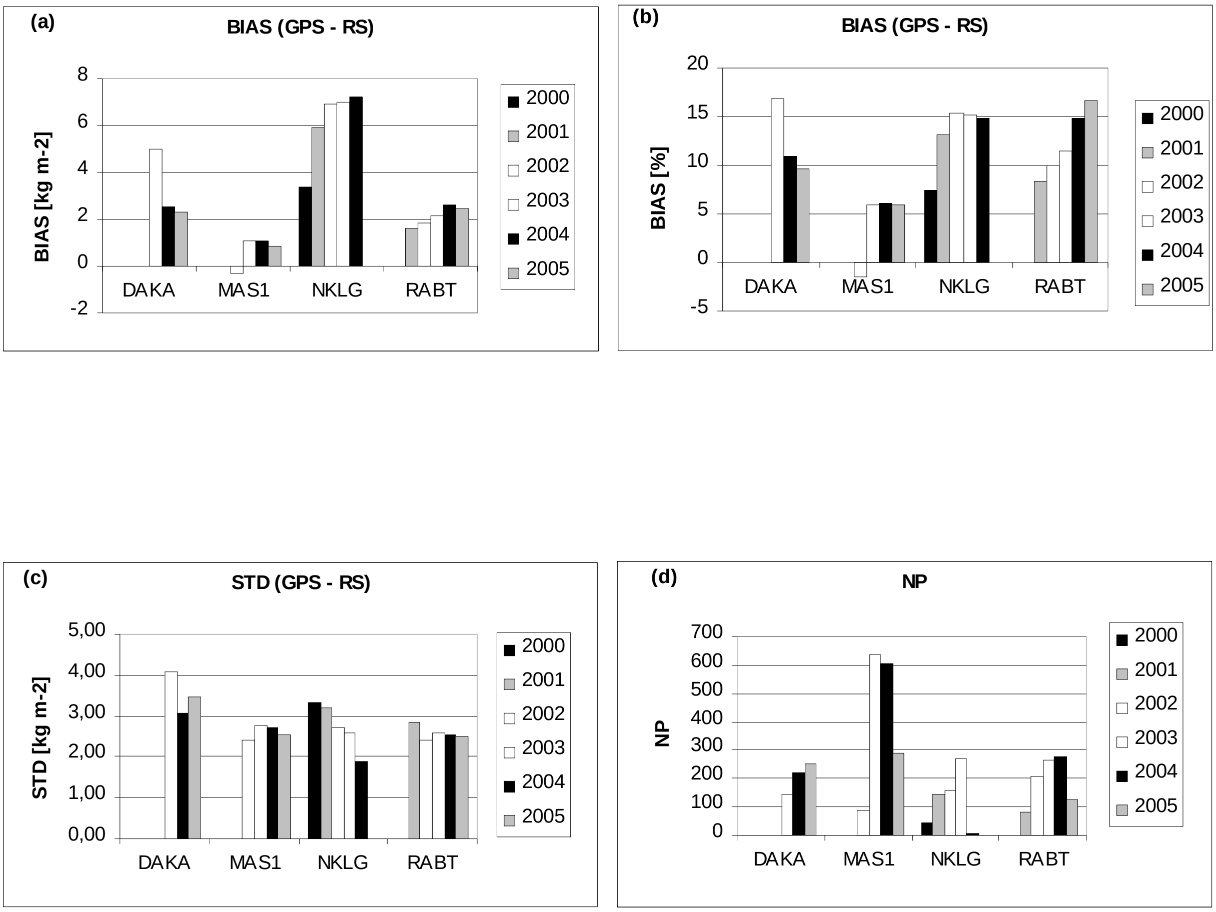

Fig. 4: Yearly statistics: (a) mean PWV differences (GPS – RS); mean relative differences (GPS – RS)/RS; (c) standard deviation; (d) number of data pairs.

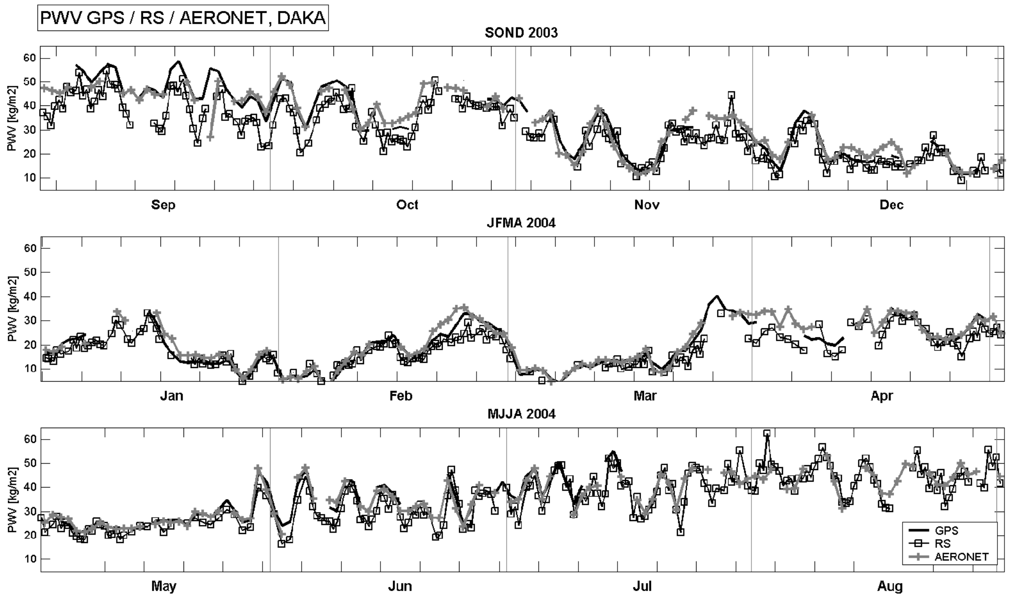

Fig. 5: Time series (01 Sept 2003 - 31 Aug 2004) of PWV estimated by GPS, RS, and AERONET sun photometers at Dakar. Grey vertical bars indicate month limits. GPS and AERONET data are daily averages. A large bias in RS PWV is detected during Sep – Oct 2003.

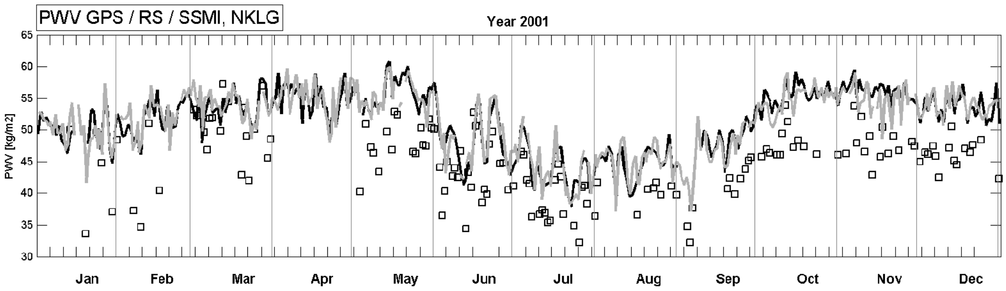

Fig. 6: Time series of PWV observed by GPS (thick black line), RS (black squares), and SSM/I (thick gray line), at station NKLG, for year 2001. GPS data are daily averages. A systematic bias is observed in RS PWV.

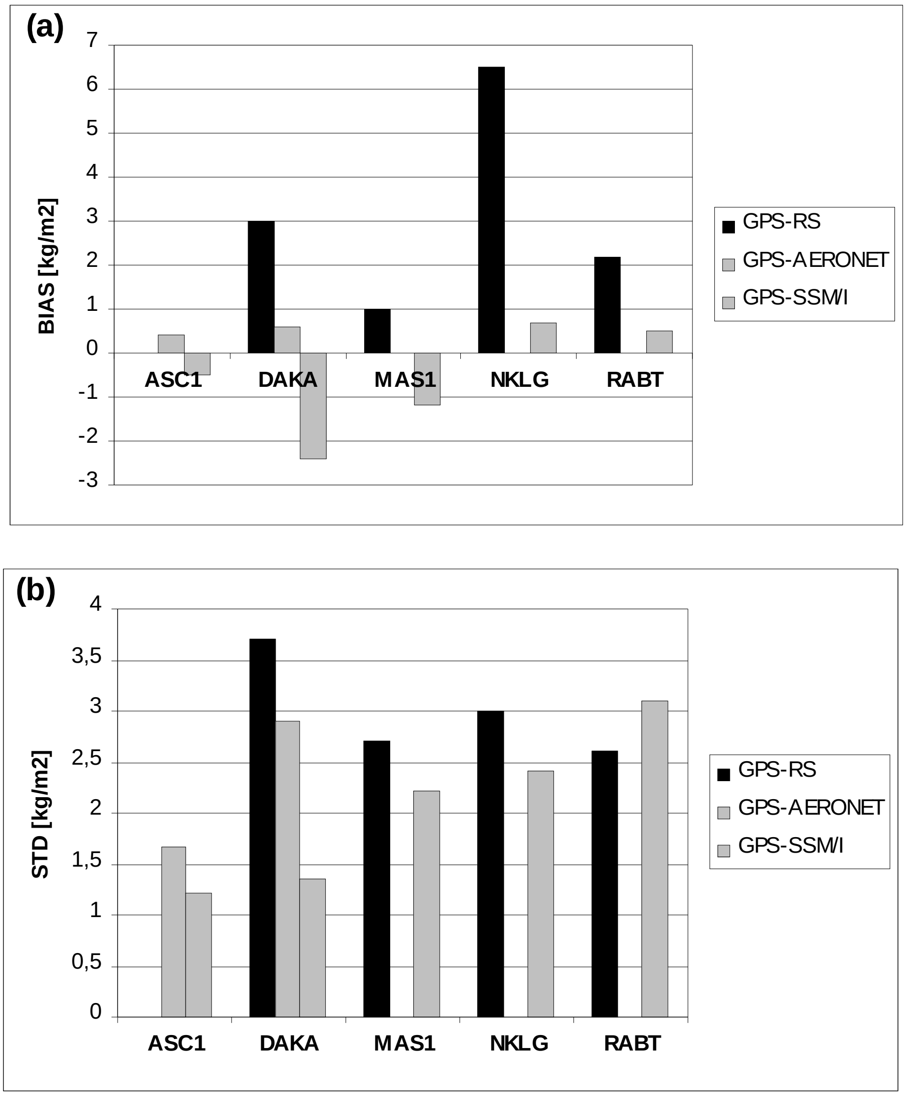

Fig. 7: Summary of inter-comparison of PWV observations: (a) mean difference and (b) standard deviation of GPS compared to the three other techniques, at five sites.

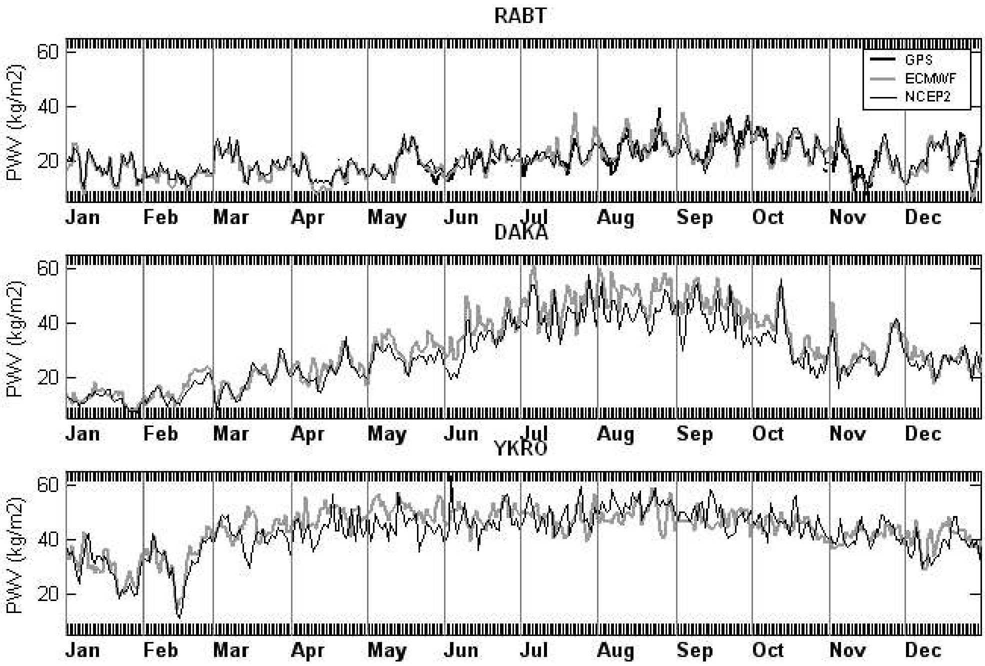
RABT
DAKA
YKRO
PWV (kg/m2)
60
40
20
GPS
ECMWF
NCEP2
Jan
Feb
Mar
Apr
May
Jun
Jul
Aug
Sep
Oct
Nov
Dec

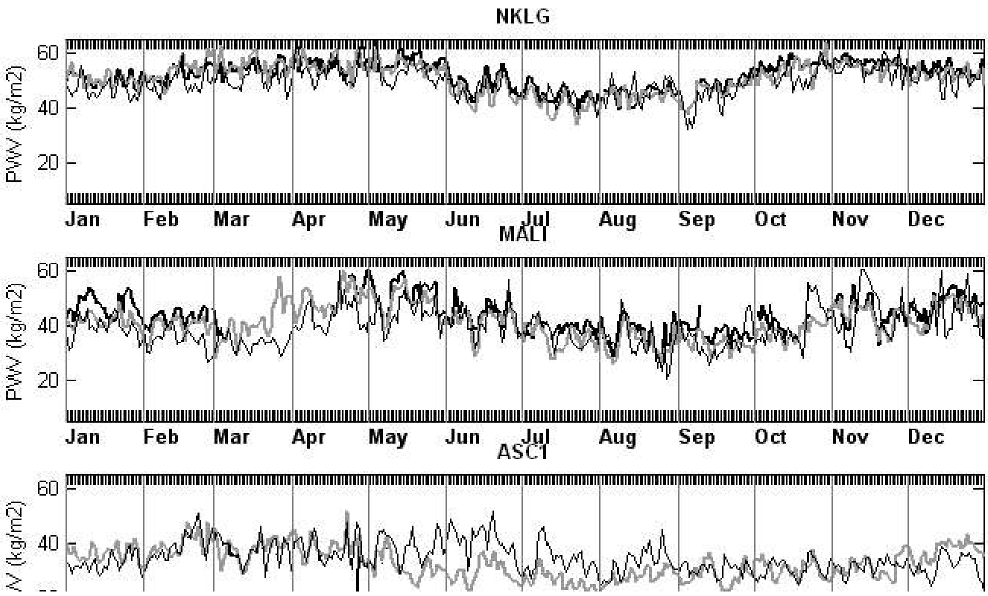
NKLG
MALI
ASC1
PWV (kg/m2)
60
40
20
Jan
Feb
Mar
Apr
May
Jun
Jul
Aug
Sep
Oct
Nov
Dec

Fig. 8: Time series of daily mean PWV from GPS (thick black line), ERA-40 (thick gray line), and NCEP2 (thin black line) for year 2001, at six sites ordered from north (RABT, 34°N) to south (ASC1, 8°S).

	GPS				**Radiosonde**			**AERONET**		**SSM/I**	**ERA40**		**NCEP2**	
Location	IGS ID	Lat. [deg]	Lon. [deg]	Alt. [m]	WMO code	Diff. Alt. [m]	Dist. [km]	Diff. Alt. [m]	Dist. [km]	Dist. [km]	Diff. Alt. [m]	Dist. [km]	Diff. Alt. [m]	Dist. [km]
Ascension Island	ASC1	-8.0	345.6	91				61	3	64	91	25	91	82
Dakar, Senegal	DAKA	14.7	342.5	16	61641	-8	6	16	63	70	-1	64	27	35
Malindi, Kenya	MALI	-3.0	40.2	53							7	90	-195	59
Mas Palomas, Spain	MAS1	27.8	344.4	156	Tenerife 60018	51	107			78	127	42	138	69
M'Barara, Ouganda	MBAR	-0.6	30.7	1349							0	78	99	106
Masuku, Gabon	MSKU	-1.6	13.6	354							-146	57	26	152
N'Koltang, Gabon	NKLG	0.4	9.7	22	Libreville 64500	7	32			126	-1	84	-159	54
Rabat, Morocco	RABT	34.0	353.1	36	60155	-22	91			100	-10	100	-246	128
Yamoussoukro, Ivory Coast	YKRO	6.9	354.8	242							47	45	-12	75

Table 1: Location and coordinates of GPS stations; distance and difference in altitude of other techniques with respect to the GPS stations (GPS – other). For SSM/I, the average nearest ocean pixel is considered. For ERA40 and NCEP2 reanalyses, fixed model grid points are used (see text for selection criteria).

	PWV [kg/m2]	BIAS [kg/m2]	BIAS [%]	STD [kg/m2]	STD [%]	Correl-ation	slope	offset [kg/m2]	NP
All RS data									
DAKA	24.9	3.0	12	3.7	15	0.96	1.14	-0.5	620
MAS1	17.2	1.0	6	2.7	16	0.91	0.96	1.6	1623
NKLG	45.6	6.5	14	3.0	7	0.81	0.76	17.3	623
RABT	18.0	2.2	12	2.6	14	0.93	1.08	0.8	960
12 UTC RS data only									
DAKA	25.2	3.5	14	3.2	13	0.97	1.14	-0.1	208
MAS1	17.3	1.0	6	2.6	15	0.91	0.98	1.4	810
NKLG	45.7	6.6	14	2.9	6	0.82	0.76	17.7	590

Table 2: Statistics of GPS - RS intercomparison at four sites; upper part uses RS data at all launching times; lower part uses only RS data at 12 UTC (at 3 sites). The columns report: average PWV from RS, mean difference (BIAS) as GPS PWV – RS PWV, standard deviation (STD) of difference, correlation between GPS PWV and RS PWV, slope and offset parameters fitted as $PWV^{GPS} = \text{slope} \times PWV^{RS} + \text{offset}$, and number of data pairs (NP).

	PWV [kg/m2]	BIAS [kg/m2]	[%]	STD [kg/m2]	[%]	Correl-ation	slope	offset [kg/m2]	NP
All data									
ASC1	31.1	0.4	1	1.7	5	0.96	1.07	-1.6	3558
DAKA	25.1	0.6	2	2.9	12	0.97	1.02	0.2	1815
11-13 UTC data only									
ASC1	31.5	-0.2	-1	1.5	5	0.97	1.06	-1.9	1082
DAKA	24.6	0.4	1	2.6	10	0.98	0.99	0.6	558

Table 3: Statistics (similar to Table 2) for GPS PWV – AERONET PWV intercomparison.

	PWV [kg/m2]	BIAS [kg/m2]	BIAS [%]	STD [kg/m2]	STD [%]	Correl-ation	slope	offset [kg/m2]	NP
ASC1	32.2	-0.5	-1	1.2	4	0.98	0.97	0.4	1615
DAKA	29.7	-2.4	-8	1.4	5	0.99	1.01	-2.6	267
MAS1	20.2	-1.2	-6	2.2	11	0.95	0.93	0.3	2411
NKLG	51.8	0.7	1	2.4	5	0.87	0.98	1.5	1637
RABT	20.5	0.5	2	3.1	15	0.90	0.92	2.1	1471

Table 4: Statistics (similar to Table 2) for GPS PWV – SSM/I PWV intercomparison.

	PWV [kg/m2]	BIAS [kg/m2]	BIAS [%]	STD [kg/m2]	STD [%]	Correl-ation	slope	offset [kg/m2]	NP
RABT	20.5	0.0	0	3.4	17	0.85	0.82	3.7	1405
MAS1	18.5	-0.3	-2	2.6	14	0.92	0.96	0.5	4146
YKRO	40.6	0.0	0	4.6	11	0.88	0.83	7.2	182
NKLG	50.7	1.1	2	4.0	8	0.77	0.63	20.1	3131
MBAR	31.1	-0.3	-1	3.3	11	0.71	0.81	5.8	1072
MSKU	44.8	1.5	3	4.0	9	0.65	0.72	14.0	1469
MALI	40.3	3.4	9	4.1	10	0.83	0.82	10.9	4609
ASC1	33.4	-1.4	-4	2.5	8	0.92	0.87	2.9	3190

Table 5: Statistics (similar to Table 2) for GPS PWV – ERA40 PWV intercomparison (6-hourly data). Stations have been ordered in decreasing latitude, from north (RABT, 34°N) to south (ASC1, 8°S).

	1000 hPa			925 hPa			1000-850 hPa	
	q_bias (g/kg)		Nobs	q_bias (g/kg)		Nobs	bias (kg/m2)	
	o-b	o-a	used/all	o-b	o-a	used/all	o-b	o-a
Rabat	-1.5	-0.9	0.40	-1.9	-0.7	0.96	-2.3	-0.9
Tenerife	-2.4	-1.7	0.78	-0.5	-0.1	0.95	-1.5	-0.8
Dakar	-1.8	-1.0	0.89	-1.9	-1.0	0.96	-2.8	-1.4
Libreville	-1.9	-1.0	0.26	-2.1	-1.1	1.00	-2.6	-1.2

Table 6: Statistics from ERA40 assimilation of RS data over period 1999-2002: specific humidity biases are reported at the two lowest levels (1000 and 925 hPa) and integrated over the 1000-850 hPa layer; o-b stands for observation minus background and o-a for observation minus analysis; Nobs is the ratio of used over all data. Stations have been ordered in decreasing latitude.

	PWV [kg/m2]	BIAS [kg/m2]	[%]	STD [kg/m2]	[%]	Correl-ation	slope	offset [kg/m2]	NP
RABT	20.4	-0.1	0	3.4	17	0.87	0.98	0.3	5102
MAS1	18.0	0.6	3	3.3	19	0.86	1.00	0.6	8206
DAKA	26.9	0.7	3	5.4	20	0.93	1.25	-6.0	1625
YKRO	45.5	-0.1	0	6.5	14	0.69	0.51	22.0	587
NKLG	49.3	3.1	6	5.2	11	0.55	0.46	29.8	6807
MBAR	27.8	2.3	8	5.3	19	0.53	0.44	17.8	2916
MSKU	42.2	4.3	10	6.0	14	0.53	0.38	30.6	2891
MALI	38.8	5.3	14	7.2	19	0.50	0.48	25.3	8115
ASC1	34.5	-2.7	-8	5.7	16	0.55	0.57	12.3	6107

Table 7: Statistics (similar to Table 5) for GPS PWV – NCEP2 PWV intercomparison (6-hourly data).

Time average	PWV [kg/m2]	BIAS [kg/m2]	[%]	STD [kg/m2]	[%]	Correl-ation	slope	offset [kg/m2]	NP
GPS - ERA40									
6-h	35.0	0.5	1	3.6	11	0.81	0.81	8.1	2401
24-h	35.0	0.6	1	2.8	9	0.87	0.86	6.1	605
7-d	34.9	0.6	1	1.9	6	0.93	0.95	2.7	94
GPS - NCEP2									
6-h	33.7	1.5	4	5.3	16	0.67	0.67	14.7	4706
24-h	33.7	1.5	4	4.8	15	0.71	0.70	13.8	1180
7-d	33.6	1.6	4	3.4	11	0.80	0.83	9.3	183

Table 8: Mean statistics (over all sites) for GPS PWV – ERA40 PWV and GPS PWV – NCEP2 PWV, for different time resolutions (6- hourly, 24-hourly, and weekly).

BIAS/STD	GPS	RS	SSM/I	ERA40	NCEP2
GPS		3.0	2.1	3.6	5.2
RS	3.2			3.2	3.8
SSM/I	-0.6			2.7	4.5
ERA40	0.5	-1.8	-0.6		4.6
NCEP2	1.6	-1.5	0.7	1.5	

Table 9: Matrix containing mean difference (BIAS) in the lower triangle and standard deviation (STD) in the upper triangle, between different PWV datasets. The difference is taken as dataset indicated in column – row. The inter-comparison between observational data (GPS, RS, and SSM/I) is computed over period Jan 1999-Jul 2005. The inter-comparison of observational data with reanalyses is limited to Jan 1999-Aug 2002.